Food Hydrocolloids 52 (2016) 732–740

Contents lists available at ScienceDirect

Food Hydrocolloids

journal homepage: www.elsevier.com/locate/foodhyd

Chitosan nanoparticles on the improvement of thermal, barrier, and mechanical properties of high- and low-methyl pectin films

Marcos Vinicius Lorevice [a, d], Caio Gomide Otoni [b, d], Márcia Regina de Moura [c, *], Luiz Henrique Capparelli Mattoso [a, b, d]

[a] PPGQ, Department of Chemistry, Federal University of São Carlos, Rodovia Washington Luís, Km 235, São Carlos, SP 13566-905, Brazil
[b] PPG-CEM, Department of Materials Engineering, Federal University of São Carlos, Rodovia Washington Luís, Km 235, São Carlos, SP 13566-905, Brazil
[c] Department of Physics and Chemistry, FEIS, São Paulo State University, Av. Brasil, 56, Ilha Solteira, SP 15385-000, Brazil
[d] LNNA, Embrapa Instrumentação, Rua XV de Novembro, 1452, São Carlos, SP 13560-970, Brazil

ARTICLE INFO

Article history:
Received 15 December 2014
Received in revised form
4 June 2015
Accepted 5 August 2015
Available online 13 August 2015

Keywords:
Biopolymer film
Pectin
Chitosan
Nanotechnology
Physical properties

Chemical compounds studied in this article:
Chitosan (PubChem CID: 71853)
Pectin (PubChem CID: 441476)
Sodium tripolyphosphate (PubChem CID: 24455)

ABSTRACT

Non-biodegradable food packaging materials have caused serious environmental problems due to their inappropriate discard. Biodegradable and renewable polymers (e.g., polysaccharides), when reinforced with nanostructures, have been used to produce novel, eco-friendly food packaging as alternatives to replace conventional packaging. This study aimed at adding chitosan nanoparticles (CSNPs) to high- (HDM) and low-methyl (LDM) pectin matrices to produce HDM pectin/CSNP and LDM pectin/CSNP nanocomposite films, as well as at evaluating the effect of CSNPs on films' mechanical, thermal, and barrier properties. Also, CSNPs were characterized as to zeta potential, average diameter, and FT-IR, whereas nanocomposites' thickness, appearance, structure, morphology, mechanical, thermal, and barrier properties were analyzed. CSNPs presented average diameter and zeta potential near to 110 nm and 50 mV, respectively. The addition of CSNPs improved the mechanical properties, being tensile strength the most affected mechanical attribute (increased from 30.81 to 46.95 MPa and from 26.07 to 58.51 MPa for HDM pectin/CSNP and LDM pectin/CSNP, respectively). These results show that the produced pectin/CSNPs nanocomposites had improved mechanical properties when compared with control pectin films, making these novel materials promising for food packaging production.

1. Introduction

The indiscriminate discard of petroleum-based food packaging has motived novel researches towards the application of eco-friendly materials in an effort to lessen the environmental impact of synthetic polymers. These novel materials are urged to (1) be obtained from renewable sources and be biodegradable, (2) present physical properties equal to or greater than conventional packaging, and (3) preserve food freshness (Haq, Hasnain, & Azam, 2014). Recent studies have proposed novel packaging produced from naturally occurring polymers (Al-Hassan & Norziah, 2012; Aydemir, Gökbulut, Baran, & Yemenicioglu, 2014; Blanco-Pascual, Goméz-Guillén, & Montero, 2014; Chiumarelli & Hubinger, 2014; Galus & Lenart, 2013; Jiménez, Fabra, Talens, & Chiralt, 2012; Kang et al., 2007; Lago-Vanzela, Nascimento, Fontes, Mauro, & Kimura, 2013; Maran, Sivakumar, Sridhar, & Immanuel, 2013; Pérez et al., 2013; Razavi, Amini, & Zahedi, 2015; Vartiainen, Tammelin, Pere, Tapper, & Harlim, 2010). According to Arora and Padua (2010), biopolymers can be classified relying upon their sources: animal-, plant-, or microbial-derived proteins, lipids, and polysaccharides, as well as polymers synthesized from natural monomers. Films and coatings have been produced from several biopolymers, including polysaccharides (Akhtar et al., 2012; Antoniou, Liu, Majeed, & Zhong, 2015; de Moura et al., 2009; Osorio, Molina, Matiacevich, Enrione, & Skurtys, 2011; Sirviö, Kolehmainen, Liimatainen, Niinimäki, & Horni, 2014) and polypeptides (Hosseini, Rezaei, Zandi, & Farahmandghavi, 2015). Those packaging materials denote feasible alternatives to replace synthetic packaging.

* Corresponding author. Department of Physics and Chemistry, FEIS, São Paulo State University, Av. Brasil, 56, Ilha Solteira, SP 15385-000, Brazil.
E-mail addresses: marcos.lorevice@gmail.com (M.V. Lorevice), caiogomide@gmail.com (C.G. Otoni), marciadqi@gmail.com (M.R. Moura), luiz.mattoso@embrapa.br (L.H.C. Mattoso).

http://dx.doi.org/10.1016/j.foodhyd.2015.08.003
0268-005X/

Chitosan (CS), a widely available, biodegradable polysaccharide derived from chitin, has been reported to produce films, coatings, and nanoparticles with antimicrobial activity (Elsabee & Abdou, 2013; Hosseini, Zandi, Rezaei, & Farahmandghavi, 2013). Pectin, naturally found on plant cell walls, has also been used to produce edible films for food packaging applications (Alves et al., 2011; Bayarri, Oulahal, Degraeve, & Gharsallaoui, 2014). According to Espitia, Du, Avena-Bustillos, Soares, and McHugh (2014), pectin is basically composed of poly α1-4-galacturonic acid. Moreira, Camargo, Marconcini, and Mattoso (2013) have reported pectin properties to vary depending upon the degree of methyl-esterification (DM), so that it is classified as high- (HDM) or low-methyl (LDM) pectin. It also exhibits biocompatibility and biodegradability (Zhang et al., 2015). However, pectin-based packaging, usually, does not match the physical properties of conventional packaging, limiting their practical application.

The addition of nanostructures into polysaccharide matrices has produced nanocomposite films with improved physical properties (Azeredo, 2009). Kanmani and Rhim (2014) reported improvements in antimicrobial properties of gelatin films after the incorporation of silver nanoparticles. Otoni et al. (2014) reported enhanced physical, mechanical, barrier, and antimicrobial properties of pectin/papaya puree-based films when essential oil nanoemulsions were added. Pectin films also presented increased mechanical and thermal properties when $Mg(OH)_2$ nanoplates were incorporated (Moreira et al., 2013). Lorevice, de Moura, Aouada, and Mattoso (2012), Martelli, Barros, de Moura, Mattoso, and Assis (2012), and de Moura, Lorevice, Mattoso, and Zucolotto (2011) added chitosan nanoparticles (CSNPs), obtained through methacrylic acid polymerization, to polysaccharide films and reported remarkably improved thermal, mechanical, and barrier properties. CSNPs formulated by ionotropic gelation (Calvo, Remuñán-López, Vila-Jato, & Alonso, 1997) have also improved the physical-chemical properties of polysaccharide-based films, such as hydroxypropyl methylcellulose (Lorevice, de Moura, & Mattoso, 2014) and tara gum (Antoniou et al., 2015). The present work aimed at formulating and characterizing CSNPs as well as producing nanocomposite HDM or LDM pectin/CSNP films with improved physical properties. The structural, mechanical, and water barrier properties of the produced films were also studied.

2. Material and methods

2.1. Material

HDM (DM > 50%, and M_w = 130.000 g·mol^{-1}) and LDM (DM < 50%, and M_w = 170.000 g·mol^{-1}) pectins were obtained from CP Kelco (Limeira, Brazil). CS (M_w = 71.300 g·mol^{-1}; deacetylation degree = 94%) was purchased from Polymar Ciência e Nutrição S/A (Fortaleza, Brazil). Sodium tripolyphosphate (TPP) and acetic acid were obtained from Sigma–Aldrich Chemical Co. (St. Louis, MO).

2.2. CSNP formulation and characterization

2.2.1. Formulation

CSNPs were formulated through ionotropic gelation of CS cationic solution with TPP anionic solution, firstly reported by Calvo et al. (1997) and then by Vimal et al. (2012, 2013). Initially, CS was dissolved in acetic acid solution to a concentration of 0.85 mg mL^{-1}, under mixing at 500 rpm for 24 h in a FISATOM 753A magnetic stirrer (Fisatom Equipamentos Científicos Ltda., São Paulo, Brazil). Then, 28 mL of a 0.11 mg mL^{-1} TPP solution were added at a rate of 1 mL min^{-1} to 70 mL of CS/acetic acid solution under mixing at 2500 rpm. Three repetitions were produced to assess formulation reproducibility.

2.2.2. Particle size, size distribution, and zeta potential

CSNP size, size distribution, and zeta potential were measured, in triplicates, through dynamic light scattering in a Zetasizer Nano ZS (Malvern Instruments Inc., Irvine, CA).

2.2.3. Infrared spectroscopy (FT-IR)

FT-IR spectra were obtained by scanning (128 scans with resolution of 2.0 cm^{-1}) CS and TPP powders and freeze-dried CSNPs (1 mg of sample plus 100 mg of KBr, mashed into pellets) at wavelengths ranging from 4000 to 600 cm^{-1}, in a Paragon 1000 infrared spectrometer (Perkin–Elmer Life and Analytical Science, Inc., Waltham, MA).

2.3. Film casting and characterization

2.3.1. Film casting

Control films of either HDM or LDM pectin were prepared by stirring a 3% (w/v) pectin aqueous solution at 2500 rpm for 24 h followed by spreading with a uniform wet thickness over a level surface and drying for 48 h at room conditions. CSNP-containing films were prepared likewise, except for the addition of 3% (w/v) of either HDM or LDM pectin to the solution obtained in CSNP formulation (item 2.2.1). All films were kept in plastic bags until used for testing.

2.3.2. Thickness

Film thicknesses were measured to the nearest 0.001 mm using a digital micrometer (Mitutoyo Corp., Kanogawa, Japan). Five random measurements per film were averaged into mean values, which were used for further calculations of mechanical and barrier properties.

2.3.3. Infrared spectroscopy (FT-IR)

FT-IR spectra were obtained by scanning (128 scans with resolution of 2.0 cm^{-1}) freeze-dried CSNPs and pectin film samples (1 mg film sample, conditioned at 0% and 50% relative humidity (RH), plus 100 mg KBr, mashed into pellets) at wavelengths ranging from 4000 to 600 cm^{-1}, in a Paragon 1000 infrared spectrometer (Perkin–Elmer Life and Analytical Science, Inc.).

2.3.4. Mechanical properties

The mechanical attributes tensile strength (TS) and elongation at break (EB) were measured according with ASTM (1997): films were cut to rectangular dimensions of 100 mm × 15 mm, equilibrated to RH of 50%, and tested in a tensile testing machine (Instron Corp., Canton, MA) fitted with a 0.01 kN load cell. Specimens were stretched at 10 mm min^{-1} from an initial gap of 50 mm until breakage. During the mechanical assay, room RH and temperature did not exceed 60% and 27 °C, respectively. TS was calculated by dividing the maximum tensile force by the cross-sectional area of the specimens, whereas EB was calculated by dividing the sample length at breakage by its initial length (50 mm) and multiplying by 100 to give percentage values.

2.3.5. Differential scanning calorimetry (DSC)

Films samples (5–8 mg) were conditioned at 50% RH for 24 h and then placed in aluminum pans and analyzed, in triplicates, in a DSC Q100 (TA Instruments, Inc.). The temperature ramped from −70 to 210 °C at a rate of 10 °C min^{-1}.

2.3.6. Water vapor transmission rate (WVTR)

WVTR was measured according with the gravimetric modified cup method, based on ASTM E96-80 (McHugh, Avena-Bustillos, &

Krochta, 1993), with a few modifications. Briefly, film samples were shaped into circles and mounted onto poly(methyl methacrylate) cups filled with deionized water, in a way that films acted as a semi-permeable barrier between a high- and a low-RH environment (held by silica). The chamber RH was maintained as low as possible during the WVTR test. The weights of the test cells were monitored throughout 24 h at 25 ± 1 °C to determine the RH at films' undersides (%), WVTR (g h^{-1} m^{-2}) and permeance (g kPa^{-1} h^{-1} m^{-2}). Two hour intervals were used between measurements to allow chamber RH to stabilize.

2.3.7. Scanning electron microscopy (SEM)

Films were analyzed by SEM in a Carl Zeiss (model Supra 35 – VP, Germany) microscope. Films had been previously kept in desiccator for 24 h, fractured in liquid nitrogen, fixed onto stubs, and coated with a gold layer (Denton Vacuum Inc., Moorestwon, NJ) for 45 s in 20 mA.

2.4. Statistical analyses

Data were analyzed through analysis of variance (ANOVA) and mean values were compared by Tukey's test at 5% of significance. Minitab (version 14.12.0) software (Minitab, Inc., State College, PA) was used.

3. Results and discussion

3.1. CSNP formulation

3.1.1. Particle size, size distribution, and zeta potential

Table 1 shows particle size, polydispersity index (PdI), and zeta potential values for three repetitions of the CSNP formulation performed in the present study. Calvo et al. (1997) showed the dependence of CSNP size on CS and TPP concentrations. de Moura et al. (2009) and Lorevice et al. (2014) indicated the same relationship between CSNP size and CS concentration. Here, the used CS concentration relied on data reported by de Moura et al. (2009, 2011), Lorevice et al. (2012, 2014). These authors found the smallest particles to show the best improvements in physical properties of polysaccharide films.

The CSNP sizes obtained in the three repetitions were equal ($p > 0.05$), though there are deviations as high as 30% (Table 1). These deviations are attributable to larger particles in suspension or particle agglomerates that were not discriminated during light scattering assays. Overall, the formulation used in the present study led to CSNPs of 94.56 ± 29.56 nm in diameter. PdI values, which indicate how size distribution is spread, also did not differ ($p > 0.05$) among the repetitions (Table 1). The formulation used here led to a mean PdI value of 0.774 ± 0.173. The constant ($p > 0.05$) particle size and PdI values in all repetitions suggest a repeatable, reproducible CSNP formulation.

The zeta potential values for the CSNP formulation are shown in Table 1. Zeta potential is a means of evaluating the stability of nanoparticles in suspension. Values higher than 20 mV (in modulus) indicate stable suspensions. The CSNPs produced here showed zeta potential values above +20 mV (Table 1), revealing highly stable suspensions. Because CS was solubilized in acetic acid solution, the amine groups (NH_2) were ionized to ionic NH_3^+ groups, leading to the positive zeta potential values observed here. This finding is in accordance to Calvo et al. (1997), Vimal et al. (2012, 2013), Lorevice et al. (2014), and Antoniou et al. (2015).

Table 1
Particle size, polydispersity index (PdI), and zeta potential values measured, in triplicates, in three repetitions of a chitosan nanoparticle synthesis.

Repetition	Particle size (nm)	PdI	Zeta potential (mV)
1	77.23 ± 32.40[a]	0.689 ± 0.223[a]	53.10 ± 1.74[a]
2	104.32 ± 39.84[a]	0.931 ± 0.119[a]	43.27 ± 1.79[b]
3	102.14 ± 13.39[a]	0.703 ± 0.007[a]	46.37 ± 4.91[ab]

[ab]Mean values ± standard deviations followed by the same lowercase superscript letters within a column are not different ($p > 0.05$).

3.1.2. Infrared spectroscopy (FT-IR)

FT-IR analyses were performed for all pectin films and freeze-dried CSNPs in order to better understand the interactions between pectin matrix and CSNP. First, the formation of CSNPs by CS and TPP groups' interactions was analyzed. CS, TPP, and CSNP spectra are shown in Fig. 1. CS powder (Fig. 1a) presented typical peaks related to its structure: 3406 cm^{-1}, associated to NH_2 stretching and presence of hydroxyl (OH) groups; the region next to 2920 and 2878 cm^{-1} was related to CH stretching; 1660 cm^{-1}, due to C═O stretching of amide I groups; 1597 cm^{-1}, credited to stretching of amide II groups; 1083 cm^{-1}, attributed to C–O stretching; and 620 cm^{-1}, related to pyranose rings. In CSNP spectrum (Fig. 1c), it is possible to observe a peak near 3465 cm^{-1}, related to hydrogen bonding system (de Moura et al., 2009); the shift of a peak originally between 1645 and 1569 cm^{-1}, indicating interactions between CS NH_3^+ groups and TPP phosphate groups; the shift of a peak originally between 1083 and 1037 cm^{-1}, showing C–O interactions with TPP; and peaks near 1213 and 1169 cm^{-1} due to P–O and P═O, respectively, stretching on TPP (Vimal et al., 2012, 2013).

3.2. Film characterization

3.2.1. Appearance

For comparison purposes, control films were produced with either HDM or LDM pectin having water as solvent. These films desirably showed handle ability, continuity, homogeneity, and transparency, whereas fractures and disruptions were absent (Fig. 2). Though Espitia et al. (2014) reported different behaviors of LDM and HDM pectins in different pH values, the DM did not affect the visual characteristics of the films (Fig. 2a and b). According to Espitia et al. (2014), when HDM pectin is added to acidic solutions, there is pectin gelation. This is not true for LDM pectin, which gels in alkaline solutions instead. Because of this, some gelation of HDM pectin was observed, but this was attenuated by using mechanical stirring at speeds higher than 1500 rpm for 12 h. The appearances

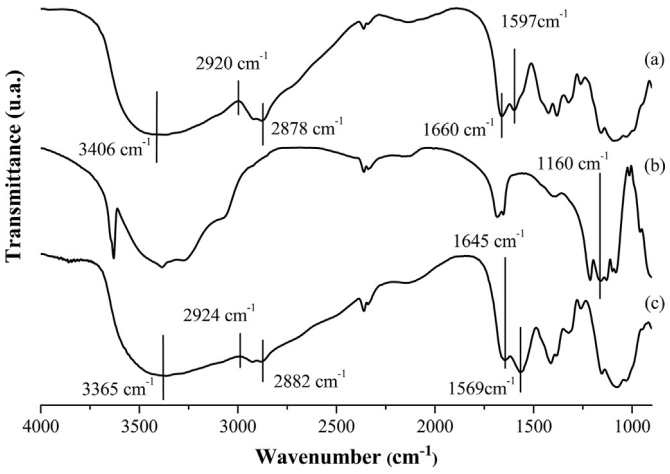

Fig. 1. Infrared spectroscopy (FT-IR) spectra of chitosan powder (a), tripolyphosphate (b), and freeze-dried chitosan nanoparticles (c).

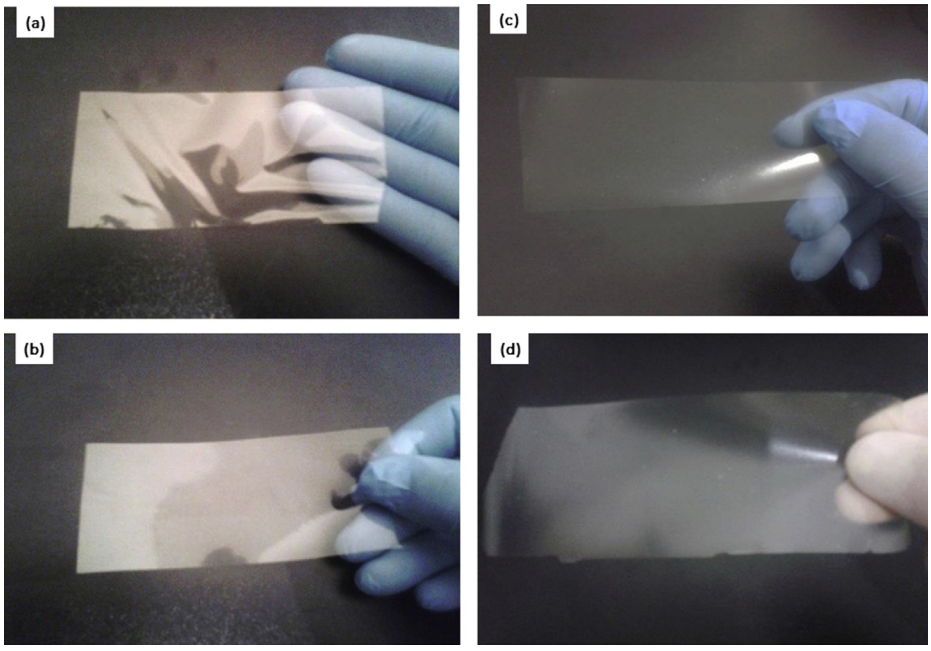

Fig. 2. Dried high- (a) or low-methyl pectin (b) films added by chitosan nanoparticles (c and d, respectively).

of HDM pectin/CSNP and LDM pectin/CSNP films after drying can be seen on Fig. 2c and d, respectively. The addition of CSNP to pectin films did not cause remarkable visual changes.

3.2.2. Thickness

Thickness values of pectin films are shown in Table 2. While pectin DM did not affect ($p > 0.05$) film thickness, films added by CSNP were thicker ($p < 0.05$) than those comprising pectin solely. This is attributable to the increased solid contents in CSNP-containing film-forming solutions when compared with pectin control films, leading to thicker dried films (Table 2).

3.2.3. Infrared spectroscopy (FT-IR)

FT-IR spectra of HDM and LDM pectins are shown in Fig. 3 and Fig. 4, respectively. The slight differences observed in both spectra are attributable to pectin esterification, given that the occurrence of methoxyl groups in galacturonic acids is dependent upon pectin DM (Espitia et al., 2014; Moreira et al., 2013), which in turn is related to the amount of carbonyl groups present in the polysaccharide molecule. Indeed, identifying carbonyl groups is a great means of differing these two pectin types. Gnanasambandam and Proctor (2000) reported the band near 1756 cm^{-1} to be related to carbonyl functional groups, and thus to pectin DM. This means of characterizing pectin DM was also described by Singthong, Cui, Ningsanond, and Goof (2004). Here, peaks near 1735 cm^{-1} can be observed in both spectra (Figs. 3 and 4), although the absorption was greater for HDM pectin than LDM pectin. The region near 1730 cm^{-1} corresponds to the number of esterified carboxyl groups, whereas the region between 1700 and 1600 cm^{-1} indicates the total number of carboxyl groups. The occurrence of methoxyl groups is then proportional to the area below the 1730 cm^{-1} peak. As expected, the area between 1730 and 1740 cm^{-1} was larger in the HDM pectin spectrum (Fig. 3) than in the LDM pectin one (Fig. 4), corroborating the higher methoxyl contents in HDM pectin than in LDM pectin.

The influence of moisture was evaluated by scanning pectin films preconditioned at 0% and 50% (Fig. 3 and Fig. 4). It was possible to notice, near to 3300 cm^{-1}, a band elongation that might indicate a strengthening of the film's interaction network. Comparing the spectra of films with and without CSNP (Fig. 3a, c, Fig. 4a, c), the different RH values promoted slight band shifts near to 3300 cm^{-1}, which was more remarkable in the spectrum of HDM pectin film conditioned at 0% RH (Fig. 3a, c, Fig. 4a, c). This region can be associated with the stretching of hydroxyl and amine groups provided by hydration degree of pectin and CS molecules. As RH was the only variable, such increase can indicate that the higher occurrence of hydroxyl groups is a result of water molecules (Fig. 3b, d, Fig. 4b, d).

There were peaks between 3400 and 2500 cm^{-1} for both HDM and LDM pectins (Figs. 3 and 4), indicating the stretching of hydroxyl groups due to intermolecular interactions through hydrogen bonding among pectin monomers (Singthong et al., 2004). Lim, Yoo, Ko, and Lee (2012) associated bands near 2930 cm^{-1} to elongation of (-O-CH_3) groups, which are present in the galacturonic acid. Here, this peak occurred near 2934 cm^{-1} for both HDM and LDM pectins (Figs. 3 and 4).

Table 2
Thickness, tensile strength (TS), and elongation at break (EB) of high- (HDM) and low-methyl (LDM) pectin films either added or not by chitosan nanoparticles (CSNP).

Film	Thickness (μm)	TS (MPa)	EB (%)
HDM pectin	25.80 ± 7.99^{ab}	30.81 ± 1.50^{a}	1.79 ± 0.27^{ab}
LDM pectin	20.60 ± 3.29^{a}	26.07 ± 3.78^{a}	0.94 ± 0.28^{a}
HDM pectin/CSNP	36.55 ± 2.19^{c}	46.95 ± 0.36^{b}	2.22 ± 0.56^{ab}
LDM pectin/CSNP	36.13 ± 2.14^{bc}	58.51 ± 11.08^{b}	2.91 ± 1.12^{b}

[abc]Mean values ± standard deviations followed by the same lowercase superscript letters within a column are not different ($p > 0.05$).

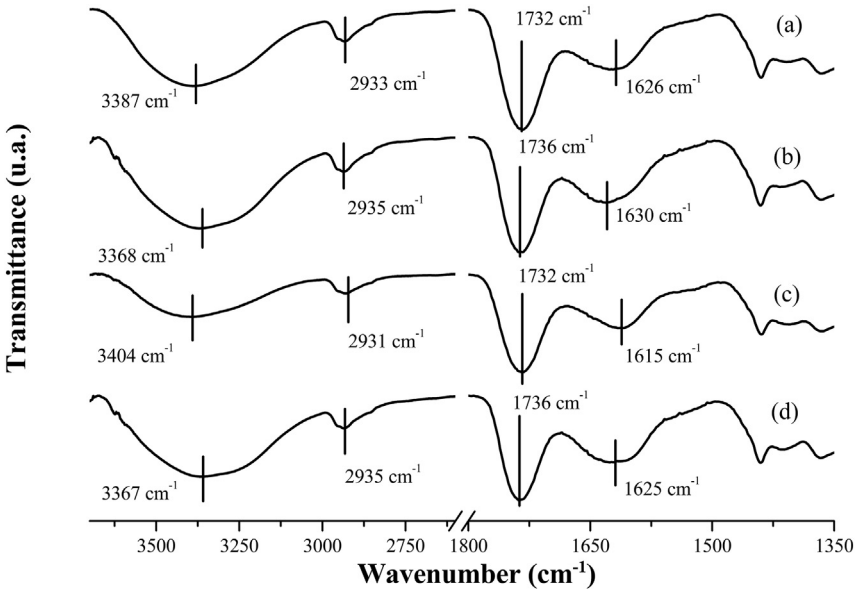

Fig. 3. Infrared spectroscopy (FT-IR) spectra of high-methyl pectin-based films added (bottom two curves) or not (top two curves) by chitosan nanoparticles. Letters *a* and *c* indicate spectra of films equilibrated at 0% RH, while letters *b* and *d* indicate spectra of films with 50% RH.

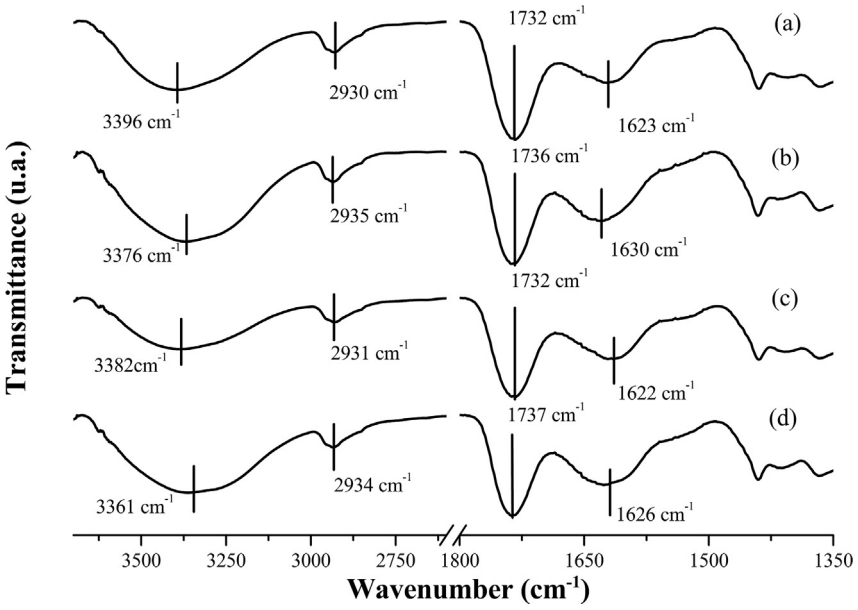

Fig. 4. Infrared spectroscopy (FT-IR) spectra of low-methyl pectin-based films added (bottom two curves) or not (top two curves) by chitosan nanoparticles. Letters *a* and *c* indicate spectra of films equilibrated at 0% RH, while letters *b* and *d* indicate spectra of films with 50% RH.

Aiming at finding interactions between CSNPs and pectin matrices, HDM pectin/CSNP and LDM pectin/CSNP nanocomposite films were analyzed by FT-IR. The spectra are shown in Figs. 3 and 4, respectively. These interactions, if detectible, can support explanations for mechanical, thermal, and barrier performances of polymer films. Pectin and hydroxypropyl methylcellulose films showed improved physical properties as a result of stronger interactions between the polymer matrices and CSNPs (Antoniou et al., 2015; Lorevice et al., 2012, 2014; Martelli et al., 2012; de Moura et al., 2009, 2011). A way of identifying interactions between CSNPs and pectin matrix is by studying changes in characteristic bands of each compound. From Figs. 3 and 4, a slight decrease in 2930 cm^{-1} band can be observed in both HDM pectin/CSNP and LDM pectin/CSNP spectra, suggesting stretching of (-O-CH_3) groups (Lim et al., 2012; Liu, Cao, Huang, Cai, & Yao, 2010). These slight changes could indicate that some amine groups from chitosan chains are interacting with pectin carbonyl groups. The stretching near to 1630 cm^{-1} can be related to COOH from pectin structure, while some shifts or decreases could suggest CSNP/pectin interactions. From Figs. 3 and 4, it is still possible to notice band decreases close to 1630 cm^{-1} when CSNPs were added. This was more remarkable in HDM pectin spectrum. A band shift was observed near to 3300 cm^{-1} in the spectrum of films conditioned at 0% RH. As there was no water interference, this shift can suggest CSNP/pectin interactions, probably between COOH and NH_3 groups. However, as CS and pectin have similar groups in their molecules,

these interactions may not be conclusive, but only a sign of CSNP/pectin interactions. It was not possible to find others changes in the HDM pectin/CSNP and LDM pectin/CSNP spectra, changes which would be useful to indicate interactions between CSNPs and pectin matrix.

3.2.4. Mechanical properties

The mechanical attributes TS and EB of HDM or LDM pectin films either added or not by CSNPs are shown in Table 2. Interestingly, pectin DM did not affect film resistance since HDM and LDM pectins led to equal ($p > 0.05$) TS values, regardless of the presence or absence of CSNP (Table 2). Our results are in accordance with those reported by Otoni et al. (2014), who found equal TS values for HDM and LDM pectin films and attributed this finding to comparable intermolecular forces stabilizing both HDM and LDM pectin chains. Contrastingly, Moreira et al. (2013) reported the DM to influence mechanical properties of pectin films, LDM values resulting in stronger and stiffer films than HDM. The authors attributed this outcome to the higher occurrence of polar groups in LDM pectin, possibly leading to higher contents of hydrogen bonds and, thus, to a more compact network.

The addition of CSNPs, however, improved ($p < 0.05$) TS of both HDM and LDM pectin films (Table 2). According to Lucas, Soares, and Monteiro (2001), low mechanical and thermal properties are caused by weak intermolecular interactions (hydrogen bonds and Van der Waals interactions) between biopolymer chains. These weak interactions result in fragile packaging, limiting their industrial applications. This has encouraged researches on novel ways of improving the mechanical properties of biopolymeric films, such as the nanocomposites reported here. By adding CSNPs, TS of pectin films was remarkably increased: HDM pectin films had an improvement of more than 50%, whereas LDM pectin films surpassed a twofold increase in TS after the addition of CSNPs (Table 2).

Reinforcement effects of CSNPs had already been reported in previous works. Antoniou et al. (2015) achieved upgraded mechanical properties when CSNP, formulated according to Calvo et al. (1997), were added to tara gum (*Cesalpinia spinosa*)-based films. The same CSNPs reinforced fish gelatin (Hosseini et al., 2015) and hydroxypropyl methylcellulose (de Moura et al., 2009) films. CSNPs formulated according to de Moura, Aouada, and Mattoso (2008) have been reported to reinforce banana-based edible films (Martelli et al., 2012). These outcomes may be explained considering the interactions between CSNPs and pectin matrices. Chang, Jian, Yu, and Ma (2010) and Martelli et al. (2012) reported particles diffused within polymer matrices and having similar intermolecular interactions to reinforce polymer films. Regarding CSNPs, the CS amine groups and pectin carboxylic groups have similar interactions, possibly producing a resistant pectin/CSNP matrix. When films are submitted to stress, chains absorb energy in different ways. Part of this energy is absorbed by bond stretching, which allows alignment of polysaccharide chains without breakage. When CSNPs are into pectin matrices, more energy is required to align polysaccharide chains. The other part of the absorbed energy is evidenced by breakage of secondary (intermolecular) interactions among polymer chains. When CSNPs are added, they are likely to be spread between adjacent chains, strengthening intermolecular interactions, decreasing chain mobility, and thus producing more resistant films. This may explain the values obtained here (Table 2).

EB is a mechanical property that gives information about how the material can deform prior to breakage. If the material is intended for food packaging applications, some deformation is required before fracturing. High EB values suggest good flexibility, extensibility, and toughness due to the cohesion among polymer chains. While pectin DM did not affect ($p > 0.05$) EB of pectin films, the addition of CSNPs appears to increase EB, though this increase was only significant ($p < 0.05$) for LDM pectin films (Table 2). The enhanced EB values of LDM pectin films incorporated with CSNPs may be explained by the higher number of interactions between this pectin and CSNP surface, given that LDM has more carboxylic groups that interact with CSNP amine groups. Moreira et al. (2013) and Otoni et al. (2014), aiming at improving the mechanical properties of polysaccharide films, reported particles, plasticizers, and others compounds added into polysaccharide matrices to change EB to higher or lower values depending on their interactions with the polymer network.

3.2.5. Differential scanning calorimetry (DSC)

DSC curves of pectin powders and films are presented in Fig. 5. The heat absorbed (ΔH, change in enthalpy) by pectin films was larger than by pectin powders. The endothermic peak temperatures (EPTs) are shown in Table 3. These temperatures were increased when pectin films were produced, but decreased when CSNPs were added. Iijima, Nakamura, Hatakeyama, and Hatakeyama (2000) and Einhorn-Stoll and Kunzek (2009) reported pectin EPTs between 100 and 150 °C, as well as associated this outcome to water present in pectin matrices. Here, EPTs were obtained within the same interval for all pectin powders and films (Table 3). The decreased EPTs and absorbed heat in CSNP-added films can be attributable to reduced natural hydration degrees of pectin films due to CSNP presence. Lower hydration degrees may result in lower chain mobility, once water can act as a plasticizing agent by imprairing films' mechanical and barriers properties. Other works have shown CSNPs to improve thermal properties of polysaccharide films (Antoniou et al., 2015; de Moura et al., 2011). Because of this, the lower EPTs found here (Table 3) suggest that CSNPs are occupying water sites within pectin matrices. This suggestion may be supported by changes in enthalpy (ΔH) in endothermic peak, which were calculated by integrating the areas below the DSC curves. These values (Table 3) showed that pectin-based films, when incorporated with CSNPs, absorbed more thermal energy than control pectin films. These higher ΔH values may support the hypothesis that CSNPs are occupying water sites in pectin matrix, replacing water molecules, decreasing the plasticizing effect caused by natural hydration, and improving thermal properties while decreasing EPT.

3.2.6. Scanning electron microscopy (SEM)

SEM images of pectin film fractures are shown in Fig. 6. Fractures aimed at noting details regarding film formation that were not detected when films' surfaces were analyzed. SEM images showing a condensed, homogeneous, and fracture- and pore-free structure suggest films with greater mechanical, thermal, and barrier properties. Control pectin films were continuous and had some degree of compression and homogeneity. HDM pectin and HDM pectin/CSNP films, however, were somehow different. HDM pectin films showed some imperfections, such as pores and factures, which might result in weaker mechanical properties. These imperfections might also lead to lower interactions among HDM pectin chains. In HDM pectin/CSNP films, CSNPs were not noticed due to their low contents in comparison with pectin. Though, CSNPs produced some changes in the films, mostly in chain density and homogeneity. The density of HDM pectin/CSNP films was previously discussed in this work, and it was also a result of intermolecular interactions between pectin network and CSNP surface. The same behavior was found when CSNPs were added into LDM pectin matrices: some factures were observed in LDM pectin films, imperfections, which were not found in LDM pectin/CSNP films. In this case, due to stronger interactions (caused by higher contents of

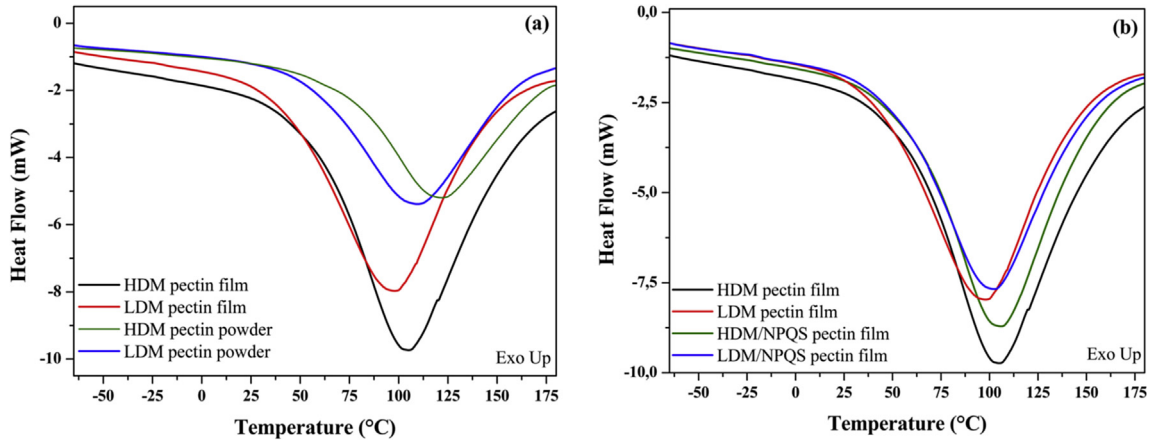

Fig. 5. Differential scanning calorimetry (DSC) curves of high- (HDM) or low-methyl (LDM) pectin powders or films either added or not by chitosan nanoparticles (CSNP).

Table 3
Water vapor transmission rate (WVTR), permeance, endothermic peak temperature and change in enthalpy in the endothermic process (ΔH) of high- (HDM) and low-methyl (LDM) pectins either as powders or films added or not by chitosan nanoparticles (CSNP).

Sample	Endothermic peak (°C)	ΔH (J g^{-1})	WVTR (g h^{-1} m^{-2})	Permeance (g kPa^{-1} h^{-1} m^{-2})
HDM pectin powder	121.8	401.6	–	–
LDM pectin powder	108.9	381.8	–	–
HDM pectin film	105.1	444.7	96.72 ± 9.60[a]	54.77 ± 10.11[a]
LDM pectin film	97.8	428.1	118.67 ± 4.60[b]	81.04 ± 7.10[b]
HDM pectin/CSNP film	105.9	547.9	97.54 ± 4.00[a]	55.10 ± 4.12[a]
LDM pectin/CSNP film	102.1	489.4	96.56 ± 2.81[a]	54.06 ± 2.79[a]

[ab]Mean values ± standard deviations followed by the same lowercase superscript letters within a column are not different ($p > 0.05$).

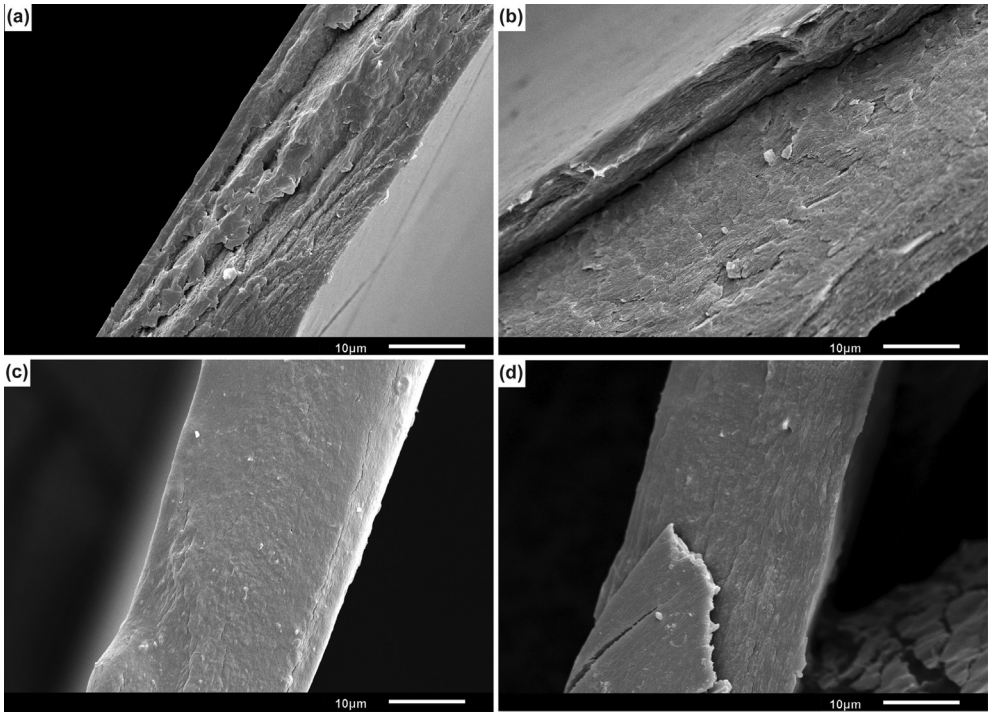

Fig. 6. Scanning electron microscopy (SEM) images of high- or low-methyl pectin films either added (b and d, respectively) or not (a and c, respectively) by chitosan nanoparticles.

carboxylic groups in LDM pectin matrices than in HDM pectin matrices), all matrices were dense and demonstrated continuity and homogeneity, causing low visual difference between LDM pectin films with or without CSNPs. The SEM images allowed noting that the addition of CSNPs did not substantially change pectin matrices, which might be a great way of producing novel nanocomposite materials.

3.2.7. Water vapor transmission rate (WVTR)

Table 3 shows WVRT and water vapor permeance of the pectin films produced here. LDM pectin films showed different ($p < 0.05$) WVTR and permeance values when compared with the other films. CSNP addition did not affect ($p > 0.05$) WVTR and permeance of HDM pectin films, but decreased ($p < 0.05$) WVTR and permeance values of LDM pectin films (Table 3).

To improve water barrier properties and boost the feasibility of applying polysaccharides for food packaging production, nanoparticles have been added to polysaccharide matrices. Different types and sizes (micro and nano) of particles were added into hydroxypropyl methylcellulose matrix, leading to decreased water vapor permeance values because particles hindered the pathway for migration of water molecules (de Moura et al., 2009). Antoniou et al. (2015) reported decreased water vapor permeability values when CSNPs were added to tara gum-based films, decrease which was correlated to CSNPs' ability to obstruct the empty spaces of the porous film matrices, generating more tortuous pathways for water molecules to diffuse. Hampered water diffusion on film matrix was also reported by Martelli et al. (2012), when CSNPs were appended on pectin-banana-films. Hosseini et al. (2015) added CSNPs to fish gelatin-based films and found water vapor permeability values to decrease mainly due to the reduction of protein matrix mobility caused by interactions between CSNP and protein chains. Yu, Wang, Hu, & Wang, 2014 reported a reduction in water permeance when montmorilonite (MMT) nanoclay was added to LDM pectin films. This behavior was related to the tortuous pathway caused by MMT nanoclay presence. On the other hand, according to Gianconi et al. (2011), not only the addition of CSNP influences water barrier properties of pectin films, but also pectin DM. These authors showed higher densities of pectin films to result in increased water vapor permeability values, while permeability to oxygen and carbon dioxide were reduced.

The results of LDM pectin films and their nanocomposites are in accordance with the observations made in FT-IR, DSC, and mechanical analyses. LDM pectin presents less methoxyl groups than HDM pectin, thus having a higher content of free hydroxyl capable of interacting with water molecules, allowing permeance by affinity of water and carboxyl groups. When CSNPs were added into the LDM pectin matrix, the surface of CSNP interacted (through its protonated amine groups) with pectin carboxyl groups (interaction suggested by the shifts and decreases in the band next to 1630 and 1730 cm^{-1} in Figs. 3 and 4), reduced number of free hydroxyl groups led to reduced WVTR and permeance values. This hypothesis is corroborated by the elongation decrease of the band near to 3300 cm^{-1} in FT-IR spectra from dried LDM pectin films when CSNP was added, region which is related to the presence of hydroxyl groups. Additionally, the increase in TS and ΔH values (Tables 2 and 3, respectively) upon CSNP addition indicates CSNP/pectin interactions and corroborates the hypothesis that CSNP decreases the number of free hydroxyl groups in LDM pectin matrices. As discussed in the literature, CSNP/interactions may be difficult the pathway available for water migration, which may result in decreased permeance and, as a result, WVTR values.

HDM pectin films, on the other hand, did not exhibit changes in WVTR and permeance values when CSNP were added. These films were a stronger barrier to water vapor than LDM pectin films. The highest DM can lead to lower interaction with water molecules due to the fact that CSNP interacted with pectin structure and did not leave hydroxyl groups available to interact with water molecules. As LDM pectin has a higher content of free hydroxyl groups than HDM pectin, the effect of reducing permeance caused by CSNP presence was more remarkable than in HDM pectin. This is in accordance with the improvement on the mechanical attributes of HDM pectin-based nanocomposites (Table 2), indicating CSNP/HDM pectin interactions. The FT-IR data of HDM pectin-based nanocomposites showed shifts and decreases in carboxyl and amine groups and also enhancements in ΔH (Table 3), suggesting CSNP/HDM pectin interactions as well.

4. Conclusions

CSNPs were formulated as nanostructures smaller than 100 nm in diameter. Their zeta potentials were higher than +20 mV, suggesting highly stable CSNP suspensions. Pectin films, comprising two pectin types (LDM and HDM), were successfully produced as homogeneous, compact, and continuous novel materials. When CSNPs were added into pectin matrices, nanocomposites were successfully formed. FT-IR suggested interactions between CS and TPP, indicating CSNP formation, as well as the interactions between CSNPs and pectin matrices, resulting in increased TS but in decreased EPT. Water permeance was affected only in the LDM pectin films, mainly due to larger interaction and solubility in water of pectin chains, since pectin is consisted of carbohydrate molecules having greater interactions with water molecules. The novel nanocomposite films developed here showed many desirable characteristics, mainly mechanical, allowing their practical application as alternatives to synthetic food packaging materials in the near future.

Acknowledgments

The authors are grateful to Embrapa Instrumentação for the infrastructure and to FINEP/MCT, CAPES, and CNPq (grant #402287/2013-4) for financial support. The authors are also thankful to Department of Physics and Chemistry, FEIS, São Paulo State University, for carrying out mechanical assays. M. V. L. (grant #2012/24362-6) and C. G. O. (grant #2014/23098-9) received scholarships from São Paulo Research Foundation (FAPESP). L. H. C. M. received scholarship from CNPq (grant #303.796/2014-6).

References

Akhtar, M. J., Jacquot, M., Jasniewski, J., Jacquot, C., Imran, M., Jamshidian, M., et al. (2012). Antioxidant capacity and light-aging study of HPMC films functionalized natural plant extract. *Carbohydrate Polymers, 89*, 1150–1158.

Al-Hassan, A. A., & Norziah, M. H. (2012). Starch-gelatin edible films: water vapor permeability and mechanical properties as affected by plasticizer. *Food Hydrocolloids, 26*, 108–117.

Alves, V. D., Castelló, R., Ferreira, A. R., Costa, N., Fonseca, I. M., & Coelhoso, I. M. (2011). Barrier properties of carrageenan/pectin biodegradable composite films. *Procedia Food Science, 1*, 240–245.

Antoniou, J., Liu, F., Majeed, H., & Zhong, F. (2015). Characterization of tara gum edible films incorporated with bulk chitosan and chitosan nanoparticle: a comparative study. *Food Hydrocolloids, 44*, 309–319.

Arora, A., & Padua, G. W. (2010). Review: nanocomposites in food packaging. *Journal of Food Science, 75*, R43–R49.

Aydemir, L. Y., Gökbulut, A. A., Baran, Y., & Yemenicioglu, A. (2014). Bioactive, functional and edible film-forming properties of isolated hazelnut *(Corylus aveliana L.)* meal proteins. *Food Hydrocolloids, 36*, 130–142.

Azeredo, H. M. C. (2009). Nanocomposites for food packaging applications. *Food Research International, 42*, 1240–1253.

Bayarri, M., Oulahal, N., Degraeve, P., & Gharsallaoui, A. (2014). Properties of lysozyme/low methoxyl (LM) pectin complexes for antimicrobial edible food packaging. *Journal of Food Science, 131*, 18–25.

Blanco-Pascual, N., Gómez-Guillén, M. C., & Montero, M. P. (2014). Integral *Mastocarpus stellatus* use for antioxidant edible film development. *Food Hydrocolloids, 40*, 128–137.

Calvo, P., Remuñán-López, C., Vila-Jato, J., & Alonso, M. (1997). Novel hydrophilic chitosan-polyethylene oxide nanoparticles as protein carriers. *Journal of Applied Polymer Science, 63*, 125–132.

Chang, P. R., Jian, R., Yu, J., & Ma, X. (2010). Fabrication and characterisation of chitosan nanoparticles/plasticised-starch composites. *Food Chemistry, 120*, 736–740.

Chiumarelli, M., & Hubinger, M. D. (2014). Evaluation of edible films and coatings formulated with cassava starch, glycerol, carnauba wax and stearic acid. *Food Hydrocolloids, 38*, 20–27.

de Moura, M. R., Aouada, F. A., Avena-Bustillos, R. J., McHugh, T. H., Krochta, J. M., &

Mattoso, L. H. C. (2009). Improved barrier and mechanical properties of novel hydroxypropyl methylcellulose edible films with chitosan/tripolyphosphate nanoparticles. *Journal of Food Engineering, 92*, 448–453.
de Moura, M. R., Aouada, F. A., & Mattoso, L. H. C. (2008). Preparation of chitosan nanoparticles using methacrylic acid. *Journal of Colloid and Interface Science, 321*, 477–483.
de Moura, M. R., Lorevice, M. V., Mattoso, L. H. C., & Zucolotto, V. (2011). Highly stable, edible cellulose films incorporating chitosan nanoparticles. *Journal of Food Science, 76*, N25–N29.
Einhorn-Stoll, U., & Kunzek, H. (2009). The influence of storage conditions heat and humidity on conformation, state transitions and degradation behavior of dried pectins. *Food Hydrocolloids, 23*, 856–866.
Elsabee, M. Z., & Abdou, E. S. (2013). Chitosan based edible films and coating: a review. *Materials Science and Engineering C, 33*, 1819–1841.
Espitia, P. J. P., Du, W.-X., Avena-Bustillos, R. J., Soares, N. F. F., & McHugh, T. H. (2014). Edible films from pectin: physical-mechanical and antimicrobial properties – a review. *Food Hydrocolloids, 35*, 287–297.
Galus, S., & Lenart, A. (2013). Development and characterization of composite edible films based on sodium alginate and pectin. *Journal of Food Engineering, 115*, 459–465.
Giancone, T., Torrieri, E., Di Pierro, P., Cavella, S., Giosafatto, V. L. C., & Masi, P. (2011). Effect of surface density on the engineering properties of high methoxyl pectin-based edible films. *Food and Bioprocess Technology, 4*, 1228–1236.
Gnanasambandam, R., & Proctor, A. (2000). Determination of pectin degree of esterification by diffuse reflectance Fourier transform infrared spectroscopy. *Food Chemistry, 68*, 327.
Haq, M. A., Hasnain, A., & Azam, M. (2014). Characterization of edible gum cordia film: effects of plasticizers. *LWT – Food Science and Technology, 55*, 163–169.
Hosseini, S. F., Rezaei, M., Zandi, M., & Farahmandghavi, F. (2015). Fabrication of bio-nanocomposite films based on fish gelatin reinforced with chitosan nanoparticles. *Food Hydrocolloids, 44*, 172–182.
Hosseini, S. F., Zandi, M., Rezaei, M., & Farahmandghavi, F. (2013). Two-step method for encapsulation of oregano essential oil in chitosan nanoparticles: preparation, characterization and *in vitro* release. *Carbohydrate Polymers, 95*, 50–56.
Iijima, M., Nakamura, K., Hatakeyama, T., & Hatakeyama, H. (2000). Phase transition of pectin with sorbed water. *Carbohydrate Polymers, 41*, 101–105.
Jiménez, A., Fabra, M. J., Talens, P., & Chiralt, A. (2012). Influence of hydroxypropylmethylcellulose addition and homogenization conditions on properties and ageing of corn starch based films. *Carbohydrate Polymers, 89*, 676–686.
Kang, H. J., Jo, C., Kwon, J. H., Kim, J. H., Chung, H. J., & Byun, M. W. (2007). Effect of a pectin-based edible coating containing green tea powder on the quality of irradiated pork patty. *Food Control, 18*, 430–435.
Kanmani, P., & Rhim, J. W. (2014). Physicochemical properties of gelatin/silver nanoparticle antimicrobial composite films. *Food Chemistry, 148*, 162–169.
Lago-Vanzela, E. S., Nascimento, P. do, Fontes, E. A. F., Mauro, M. A., & Kimura, M. (2013). Edible coating from native and modified starches retain carotenoids in pumpkin during drying. *LWT – Food Science and Technology, 50*, 420–425.
Lim, J., Yoo, J., Ko, S., & Lee, S. (2012). Extraction and characterization of pectin from Yuza *(Citrus junos)* pomace: a comparison of conventional-chemical and combined physical-enzymatic extractions. *Food Hydrocolloids, 29*, 160–165.
Liu, L., Cao, J., Huang, J., Cai, Y., & Yao, J. (2010). Extraction of pectins with different degrees of esterification from mulberry branch bark. *Bioresource Technology, 101*, 3268–3273.
Lorevice, M. V., de Moura, M. R., Aouada, F. A., & Mattoso, L. H. C. (2012). Development of novel guava puree films containing chitosan nanoparticles. *Journal of Nanoscience and Nanotechnology, 12*, 2711–2718.
Lorevice, M. V., de Moura, M. R., & Mattoso, L. H. C. (2014). Nanocomposite of papaya puree and chitosan nanoparticles for application in packaging. *Química Nova, 37*, 931–936.
Lucas, E. F., Soares, B. G., & Monteiro, E. (2001). *Caracterização de Polímeros: Determinação de Peso Molecular e Análise Térmica*. Rio de Janeiro: E-papers.
Maran, J. P., Sivakumar, V., Sridhar, R., & Immanuel, V. P. (2013). Development of model for mechanical properties of tapioca starch based edible films. *Industrial Crops and Products, 42*, 159–168.
Martelli, M. R., Barros, T. T., de Moura, M. R., Mattoso, L. C. H., & Assis, O. B. G. (2012). Effect of chitosan nanoparticles and pectin content on mechanical properties and water permeability of banana puree films. *Journal of Food Science, 78*, N98–N104.
McHugh, T. H., Avena-Bustillos, R. J., & Krochta, J. M. (1993). Hydrophilic edible films: modified procedure for water vapor permeability and explanation of thickness effects. *Journal of Food Science, 58*, 899–903.
Moreira, F. K. V., de Camargo, L. A., Marconcini, J. M., & Mattoso, L. H. C. (2013). Nutraceutically inspired pectin-$Mg(OH)_2$ nanocomposites for bioactive packaging applications. *Journal of Agricultural and Food Chemistry, 61*, 7110–7120.
Osorio, F. A., Molina, P., Matiacevich, S., Enrione, J., & Skurtys, O. (2011). Characteristics of hydroxy propyl methyl cellulose (HPMC) based edible film developed for blueberry coatings. *Procedia Food Science, 1*, 287–293.
Otoni, C. G., de Moura, M. R., Aouada, F. A., Camilloto, G. P., Cruz, R. S., Lorevice, M. V., et al. (2014). Antimicrobial and physical-mechanical properties of pectin/papaya puree/cinnamaldehyde nanoemulsion edible composite films. *Food Hydrocolloids, 41*, 188–194.
Pérez, C. D., De'Nobili, M. D., Rizzo, S. A., Gerschenson, L. N., Descalzo, A. M., & Rojas, A. M. (2013). High methoxyl pectin-methyl cellulose films with antioxidant activity at a functional food interface. *Journal of Food Engineering, 116*, 162–169.
Razavi, S. M. A., Amini, A. M., & Zahedi, Y. (2015). Characterization of a new biodegradable edible film based on sage seed gum: influence of plasticizer type and concentration. *Food Hydrocolloids, 43*, 290–298.
Singthong, J., Cui, S. T., Ningsanond, S., & Goff, H. D. (2004). Structural characterization, degree of esterification and some gelling properties of Krueo Ma Noy (*Cissampelos pareira*) pectin. *Carbohydrate Polymers, 58*, 391–400.
Sirviö, J. A., Kolehmainen, A., Liimatainen, H., Niinimäki, J., & Horni, O. E. O. (2014). Biocomposite cellulose-alginate films: promising packaging materials. *Food Chemistry, 151*, 343–351.
Vartiainen, J., Tammelin, T., Pere, J., Tapper, U., & Harlim, A. (2010). Biohybrid barrier films from fluidized pectin and nanoclay. *Carbohydrate Polymers, 82*, 989–996.
Vimal, S., Abdul Majeed, S., Taju, G., Nambi, K. S. N., Sundar Raj, N., Madan, N., et al. (2013). Chitosan tripolyphosphate (CS/TPP) nanoparticles: preparation, characterization and application for gene delivery in shrimp. *Acta Tropica, 128*, 486–493.
Vimal, S., Taju, G., Nambi, K. N. S., Abdul Majeed, S., Sarath Babu, V., Ravi, M., et al. (2012). Synthesis and characterization of CS/TPP nanoparticles for oral delivery of gene in fish. *Aquaculture, 358–359*, 14–22.
Yu, W.-Y., Wang, Z.-W., Hu, C.-Y., & Wang, L. (2014). Properties of low methoxyl pectin-carboxymethyl cellulose based on montmorillonite nanocomposite films. *International Journal of Food Science & Technology, 49*, 2592–2601.
Zhang, T., Zhou, P., Zhan, Y., Shi, X., Lin, J., Du, Y., et al. (2015). Pectin/lysozyme bilayers layers-by-layer deposited cellulose nanofibrous mat for antibacterial application. *Carbohydrate Polymers, 117*, 687–693.